Appendix A

Simulation of SAR images

A.1 Simulation of Spatially Correlated Speckle

The point spread function (PSF) of the SAR system induces a spatial correlation in the speckle in uniform regions. In order to simulate speckle with the same characteristics as the speckle found in the SAR image we therefore also need to simulate this correlation effect. If the PSF of the system is known, the complex speckle image can be convolved with this PSF. If the PSF is not known we can simulate correlated speckle in the following manner.

The underlying hypotheses are that the speckle is fully-developed and that it is white; i.e. that its spectral density is constant. We start by finding a region with fully-developed speckle in the SLC SAR image. Of this region an FFT is calculated along x and y direction. This yields the spectral density of the correlated speckle (S_{CS}) along x and y-direction, for which [23]:

$$\begin{aligned} S_{CS,x} &= S_{US,x} H_x^2, \\ S_{CS,y} &= S_{US,y} H_y^2. \end{aligned} \tag{A.1}$$

with $S_{US,x}$ the spectral density of the uncorrelated speckle (which is a constant for white speckle), $S_{CS,y}$ the spectral density of correlated speckle and H the transfer function of the SAR system.

From this, H can be found, upto a constant, and a 2D filter in the spectral domain can be constructed. Normalising this filter in energy, i.e. ensuring that the sum of the squared coefficients is equal to one, gives the transfer function of the system.

This can now be used to generate correlated speckle. First uncorrelated speckle is generated with a variance of 0.5. This is done by random sampling of a normal distribution with zero mean and variance=0.5.

In this way the real and imaginary component of an image with uncorrelated speckle is generated.

These images are transformed into the fourier domain and both are pixel-wise multiplied with the transfer function.

Inverse FFT gives the two components of the complex correlated speckle image. This is normalised by dividing through the standard deviation.

An image can now be generated by multiplying the speckle image with a given ideal image (i.e. consisting of patches of constant value corresponding the wanted radar reflectivity).

Note that the method described above is only correct in uniform regions of the image. If the ideal image contains edges, the PSF of the SAR image will also smooth these edges and therefore the ideal image has to be convolved with the PSF before the spatially correlated speckle is added to it. However we only used the procedure described above to generate "uniform" images to determine the probability of false alarms as a function of the threshold and therefore the method is valid. Only in the case where the ROC curves as a function of contrast level in simulated images are determined (see e.g. fig 5.18), the procedure is, strictly speaking, not valid. However, because of the sub-sampling in the scanning rectangles that is used in the various edge detectors, the influence of the error is negligable.

A.2 Introducing Interchannel Correlation

In order to introduce interchannel correlation, the random generation step for creating the real and imaginary components of uncorrelated speckle must be linked between the different channels (different polarisations).

Therefore we start by generating a real image of the first channel and from this all other channels are determined by introducing a pixel-wise dependency into the random generation. In each pixel the random generation depends on the corresponding pixel in the start image, on the correlation between the two images and on their respective radar reflectivity. If σ_i is the standard deviation of the speckle in the start image and $C(i,j)$ the inter-channel correlation coefficient between channels i and j then the image of channel j can be derived as:

$$\begin{aligned} \sigma_j &= \sqrt{1 - C_{i,j}^2} * \sigma_i \\ \mu_j(x,y) &= C_{i,j} * \frac{\sigma_j}{\sigma_i} * Im_i(x,y) \end{aligned} \tag{A.2}$$

Pick a value randomly from a normal distribution with average $\mu_j(x,y)$ and standard deviation σ_j. The result is the value of image j at position x,y: $Im_j(x,y)$.

Appendix B

Pulse Compression

To understand how a matched filter can be used to compress a pulse waveform we will first derive the expression of a matched filter and then apply it to a frequency modulated signal.

B.1 The Matched Filter

The matched filter is a linear filter that maximizes the signal to noise ratio at its output stage. The matched filter is designed to filter a signal that was corrupted by additive noise. In fig. B.1 s(t) is the original signal and n(t) is the noise (with mean power density N_p). The noise is added to the signal to yield the corrupted signal x(t). The idea is to design a filter with an impulse response h(t) such that, applying this filter to x(t) gives a new signal y(t) that is optimal in some sense.

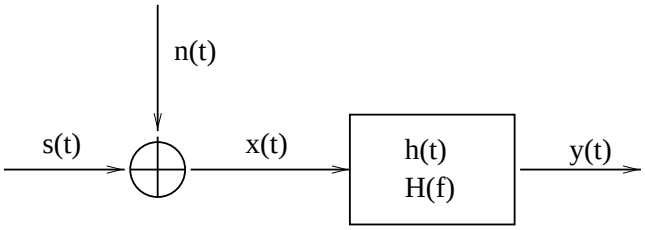

Figure B.1: Linear Filter

The effect of applying the linear filter h(t) to the corrupted signal x(t) is a convolution in the time-domain given by:

$$y(t) = x(t) * h(t) = \int_{-\infty}^{+\infty} x(\tau)h(t-\tau)d\tau \tag{B.1}$$

The frequency response of a linear filter h(t) is the Fourier transform of h(t):

$$H(f) = \int_{-\infty}^{+\infty} h(t)exp(-i2\pi ft)dt \tag{B.2}$$

The inverse transform is:

$$h(t) = \int_{-\infty}^{+\infty} H(f) exp(i2\pi ft) df \tag{B.3}$$

It then follows from the properties of the Fourier transform that:

$$y(t) = \int_{-\infty}^{+\infty} X(f)H(f) exp(i2\pi ft) df \tag{B.4}$$

where X(f) is the Fourier transform of x(t). As said previously the matched filter maximizes the signal to noise ratio (SNR) at the output stage. We define the SNR as:

$$SNR = \frac{S}{N} = \frac{\text{Peak Output Signal Power}}{\text{Average Noise Power}} \tag{B.5}$$

Suppose that the maximal peak output level *due to the signal alone* occurs at some time t_0. Then:

$$S = \mid y_s(t_0) \mid^2 = \mid \int_{-\infty}^{+\infty} S(f)H(f) exp(i2\pi ft_0) df \mid^2 \tag{B.6}$$

Now suppose that the noise is white over a bandwidth (-W,W) with a mean power density N_p. The average noise power is:

$$N = E\left[\mid y_n(t) \mid^2\right] = E\left[\mid \int_{-\infty}^{+\infty} n(\tau)h(t-\tau)d\tau \mid^2\right] \tag{B.7}$$

For a white noise this can be shown to result in:

$$N = \frac{N_p}{2} \int_{-\infty}^{+\infty} \mid H(f) \mid^2 df \tag{B.8}$$

Thus:

$$SNR = \frac{S}{N} = \frac{\mid \int_{-\infty}^{+\infty} S(f)H(f) exp(i2\pi ft) df \mid^2}{\frac{N_p}{2} \int_{-\infty}^{+\infty} \mid H(f) \mid^2 df} \tag{B.9}$$

By using Schwarz' inequality for integrals we obtain for the nominator:

$$\begin{aligned} \mid \int_{-\infty}^{+\infty} S(f)H(f) exp(i2\pi ft) df \mid^2 &\leq \int_{-\infty}^{+\infty} \mid S(f) exp(i2\pi ft) \mid^2 df \int_{-\infty}^{+\infty} \mid H(f) \mid^2 df \\ &= \int_{-\infty}^{+\infty} \mid S(f) \mid^2 df \int_{-\infty}^{+\infty} \mid H(f) \mid^2 df \end{aligned} \tag{B.10}$$

This gives an upper limit for the nominator and thus also for the SNR. The maximal SNR that can be reached is thus:

$$SNR_{max} = \frac{2}{N_p} \int_{-\infty}^{+\infty} \mid S(f) \mid^2 df \tag{B.11}$$

The integral in this expression is the energy of the signal. The maximal signal to noise ratio that can be obtained thus only depends on the signal energy and the noise power density and is independent of the waveform that is used.

The maximum SNR (the equality in equation B.10) is reached when:

$$H(f) = mS^*(f)exp(-i2\pi f t_0) \tag{B.12}$$

where m is an arbitrary constant. The equivalent equation in the time-domain is

$$h(t) = mS^*(t_o - t) \tag{B.13}$$

The impulse response of the matched filter is thus a time-reversed version of the complex conjugate of the input signal s(t).

B.2 Matched Filter for the Chirp

Let us now apply this to the chirp as defined in eq. 2.4. The matched filter for the chirp is thus:

$$h(t) = mAexp\left[-i2\pi\left(f_0(t_0 - t) + \frac{1}{2}\alpha(t_0 - t)^2\right)\right] \tag{B.14}$$

The output of the matched filter in the presence of the input signal alone (no noise) is thus:

$$\begin{aligned}
y_s(t) &= \textstyle\int_{-\infty}^{+\infty} p(\tau)h(t-\tau)d\tau \\
&\qquad \text{set } t_0 = 0 \text{ and } A = \tfrac{1}{m} \\
&= A\textstyle\int_{-\frac{\tau_p}{2}}^{+\frac{\tau_p}{2}} exp\left[i2\pi(f_0\tau + \frac{1}{2}\alpha\tau^2)\right] exp\left[-i2\pi(f_0(\tau - t) + \frac{1}{2}\alpha(\tau - t)^2)\right] d\tau \\
&= A\textstyle\int_{-\frac{\tau_p}{2}}^{+\frac{\tau_p}{2}} exp\left[i2\pi(f_0 t + \frac{1}{2}\alpha\tau^2 - \frac{1}{2}\alpha(\tau - t)^2)\right] d\tau \\
&= A\textstyle\int_{-\frac{\tau_p}{2}}^{+\frac{\tau_p}{2}} exp\left[i2\pi(\alpha\tau t + f_0 t - \frac{1}{2}\alpha t^2)\right] d\tau \\
&= Aexp\left[i2\pi(f_0 t - \frac{1}{2}\alpha t^2\right] \textstyle\int_{-\frac{\tau_p}{2}}^{+\frac{\tau_p}{2}} Aexp\left[i2\pi\alpha\tau t\right] d\tau \\
&= Aexp\left[i2\pi(f_0 t - \frac{1}{2}\alpha t^2\right] \frac{sin(\pi\alpha t\tau_p)}{\pi\alpha t} \\
&= A\tau_p exp\left[i2\pi(f_0 t - \frac{1}{2}\alpha t^2\right] sinc(\pi\alpha t\tau_p)
\end{aligned} \tag{B.15}$$

The result is thus a replica of the emitted signal but windowed by a sinc function. The sinc function can thus be seen as limiting the actual pulse duration. The pulse duration τ_{eff} after demodulation is by convention set to the time between the two first zeros of the

sinc which is $\tau_{eff} = 1/\alpha\tau_p$. $\alpha\tau_p$ is the bandwidth B_p of the modulation that was applied, thus $\tau_{eff} = 1/B_p$.

Appendix C

Correction Factors for the Edge Detectors

C.1 Variance of the Mean

In the contour detector described in section 5.3.1 the variance of the mean is deduced from the variance of the samples. For spatially correlated observations within the sample, a correction factor is introduced in eq. 5.15. In the following eq. 5.15 is proven.

Lets start with the 1-dimensional case. Suppose we have a 1D signal from which a part is digitised to give a set of n points $x_1, ..., x_n$ (observations) which correspond to succesive values of the signal. The observations are spatially (or temporally) correlated and we would like to determine how this correlation affects the variance of the mean of the samples.

The variance (standard error) of the mean is given by:

$$\begin{aligned} var(\overline{x}) &= E\left\{\overline{x} - \mu\right\}^2 \\ &= E\left\{\frac{1}{n}\sum_{i=1}^{n} x_i - \mu\right\}^2 \\ &= \frac{1}{n^2} E\left\{(\sum_{i=1}^{n} x_i)^2 - 2n\mu\sum_{i=1}^{n} x_i + n^2\mu^2\right\} \\ &= \frac{1}{n^2} E\left\{\sum_{i=1}^{n} x_i^2 + \sum_{i=1}^{n}\sum_{j=1, j\neq i}^{n}(x_i x_j)\right\} - n^2\mu^2 \\ &= \frac{1}{n^2}\left[\sum_{i=1}^{n} E\left\{x_i^2\right\} + \sum_{i=1}^{n}\sum_{j=1, j\neq i}^{n} E\left\{(x_i x_j)\right\} - n^2\mu^2\right] \end{aligned} \tag{C.1}$$

If the observations are not correlated $E(x_i x_j) = E(x_i)E(x_j)$ and thus:

$$\begin{aligned} var(\overline{x}) &= \frac{1}{n^2}\left[nE(x^2) + n(n-1)\mu^2 - n^2\mu^2\right] \\ &= \frac{1}{n}\left[E(x^2) - \mu^2\right] \end{aligned} \tag{C.2}$$

This is equal to the variance of the samples divided by n:

$$\begin{aligned} var(x) &= E\{x-\mu\}^2 \\ &= \tfrac{1}{n}\textstyle\sum_{i=1}^{n}(x_i-\mu)^2 \\ &= \tfrac{1}{n}\textstyle\sum_{i=1}^{n}(x_i^2-2\mu x_i+\mu^2) \\ &= \tfrac{1}{n}\textstyle\sum_{i=1}^{n}(x_i^2)-\mu^2 \\ &= E(x^2)-\mu^2 \end{aligned} \tag{C.3}$$

This well known result for independent observations is not valid when the observations are correlated. In that case the term $\sum_{i=1}^{n}\sum_{j=1,j\neq i}^{n} E\{(x_i x_j)\}$ can be evaluated as follows: The spatial correlation coefficient is defined as a function of the lag between the observations:

$$\rho(k) = \frac{E\{(x_i-\mu)(x_{i-k}-\mu)\}}{var(x)} \tag{C.4}$$

and

$$\begin{aligned} E\{(x_i-\mu)(x_{i-k}-\mu)\} &= E\{x_i x_{i-k}\}-\mu E\{x_{i-k}\}-\mu E\{x_i\}+\mu^2 \\ &= E\{x_i x_{i-k}\}-\mu^2 \end{aligned} \tag{C.5}$$

and thus $E\{x_i x_{i-k}\}-\mu^2 = \rho(k)var(x)$

It is thus possible to express the second term in the last line of eqs. C.1 as a function of the correlation coefficients at different lags by regrouping the terms (as a function of the lags).

Note that there are $n-i$ terms at lag $+i$ (and the same number at $-i$) in the sum (see fig. C.1).

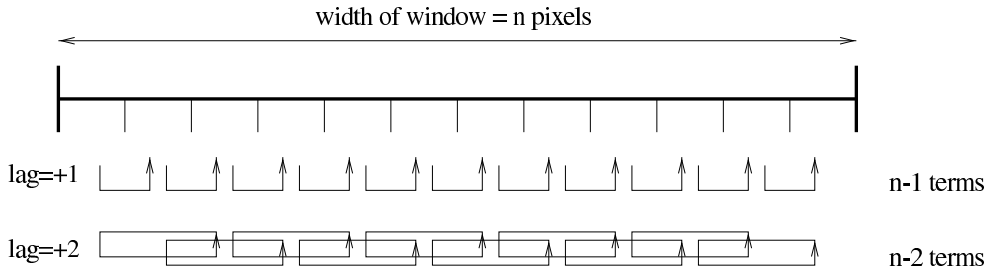

Figure C.1: Vectorised edges

$$\begin{aligned}\sum_{i=1}^{n}\sum_{j=1,j\neq i}^{n} E\{(x_i x_j)\} &= \sum_{i=2}^{n} E\{x_i x_{i-1}\} + \sum_{i=1}^{n-1} E\{x_i x_{i+1}\} \\ &+ \sum_{i=3}^{n} E(\{x_i x_{i-2}\} + \sum_{i=1}^{n-2} E\{x_i x_{i+2}\} \\ &+ \sum_{i=4}^{n} E(\{x_i x_{i-3}\} + \sum_{i=1}^{n-3} E\{x_i x_{i+3}\} \\ &+ ... \\ &= \sum_{i=1}^{n-1}[2(n-i)(\rho(i)var(x)+\mu^2)] \\ &= n(n-1)\mu^2 + var(x)\sum_{i=1}^{n-1}[2(n-i)(\rho(i)]\end{aligned} \tag{C.6}$$

Here, the hypothesis in the penultimate step was that $\rho(i) = \rho(-i)$. Noting that $n^2\mu^2 = n\mu^2 + n(n-1)\mu^2$ we can now write:

$$\begin{aligned}var(\overline{x}) &= \tfrac{1}{n^2}\left[\sum_{i=1}^{n} E\{x_i^2\} - n\mu^2 + \sum_{i=1}^{n}\sum_{j=1,j\neq i}^{n} E\{(x_i x_j)\} - n(n-1)\mu^2\right] \\ &= \tfrac{1}{n}\left[E\{x^2\} - \mu^2 + \tfrac{var(x)}{n}\sum_{i=1}^{n-1}[2(n-i)(\rho(i)]\right] \\ &= \tfrac{var(x)}{n}\left\{\rho(0) + \sum_{i=1}^{n-1}\left[2(1-\tfrac{i}{n})(\rho(i)\right]\right\}\end{aligned} \tag{C.7}$$

because $E(x^2) - \mu^2 = \rho(0)var(x)$.

In case of a uni-variate two-dimensional signal, the observations are the elements of a rectangular window. For sampling in a rectangular window with width W and height H one finds in a similar way as above, by groupng the cross-terms as a funcion the 2D correlation function that:

$$var(\overline{x}) = \tfrac{var(x)}{n}\left\{\rho(0) + \sum_{i=1}^{W-1}\sum_{j=1}^{H-1}\left[2(1-\tfrac{i}{W})(1-\tfrac{j}{H})(\rho(i,j)\right]\right\} \tag{C.8}$$

In eq. 5.15 the hypothesis is made that the spatial correlation along azimuth and range direction are independent:

$$\rho(i,j) = \rho_H(i)\rho_V(j) \tag{C.9}$$

in which ρ_H and ρ_V are the spatial correlation function in horizontal and vertical direction respectively.

Please note that the correction factor depends on the orientation of the windows. For rectangular windows with the sides along the x and y-axes in the image, the correction factor derived above applies. If the windows are rotated over an angle θ, the coordinates of the correlation function need to be rotated too:

$$\rho_\theta(i,j) = \rho_{H,\theta}(i)\rho_{V,\theta}(j) = \rho_H(i\ \cos\theta - j\ sin\theta)\rho_V(i\ sin\theta + j\ \cos\theta) \tag{C.10}$$

The spatial correlation in a SAR image is due to two factors. The first is the effect of the impulse response of the SAR procesing. For this term the correlation in azimuth

and range are independent and this correlation depends only on the SAR system and is independent of the position in the image. However, the second factor in the spatial correlation of a SAR image is caused by texture, e.g. a pattern in the scattering of the terrain. It is therefore only possible to find a correction factor for the variance of means in non-textured regions. A contour detector incorporating the correction factor would thus necessarily still give more false alarms in textured regions because the correction will still be too small. Please note that an approach based on subsampling will have the same problem. However, if random subsampling is used, the probability of finding false alarms at neighbouring positions should be lower than when the correction factor is explicitely used in the detector and no subsampling is applied. On the other hand, in regions without texture, applying the correction factor would avoid the need for subsampling and thus enable one to use smaller scanning windows.

C.2 Covariance of the Mean

In the Hotellings test and the Levene test the covariance matrix between the different channels is used. We have seen that the obtained statistics are too large. In fact, the Hotellings test is based on the hypothesis of (spatially) independent observations and the fact that, in that case, the covariance of the mean is equal to that of the samples divided by the sample size. In the following the error that is made by neglecting the spatial correlation between the observations is determined. Therefore the influence of the spatial correlation on the covariance of the mean is determined. Lets determine an expression for each element of the covariance matrix. Let P and Q denote two channels (e.g. spectral bands or polarisations), the covariance of the mean between channels P and Q is:

$$\begin{aligned}
cov(\overline{x_P}, \overline{x_Q}) &= E\left\{(\overline{x_P} - \mu_P)(\overline{x_Q} - \mu_Q)\right\}^2 \\
&= E\left\{(\tfrac{1}{n}\textstyle\sum_{i=1}^{n} x_{i,P} - \mu_P)(\tfrac{1}{n}\sum_{i=1}^{n} x_{i,Q} - \mu_Q)\right\} \\
&= \tfrac{1}{n^2} E\left\{\textstyle\sum_{i=1}^{n} x_{i,P}x_{i,Q} + \sum_{i=1}^{n}\sum_{j=1,j\neq i}^{n}(x_{i,P}x_{j,Q})\right\} \\
&-\tfrac{1}{n}\mu_P \textstyle\sum_{i=1}^{n} E\{x_{i,Q}\} - \tfrac{1}{n}\mu_Q \sum_{i=1}^{n} E\{x_{i,P}\} + \mu_P\mu_Q \\
&= \tfrac{1}{n}\left\{\tfrac{1}{n}\textstyle\sum_{i=1}^{n} E\{x_{i,P}x_{i,Q}x_i\} - n\mu^2 + \tfrac{1}{n}\sum_{i=1}^{n}\sum_{j=1,j\neq i}^{n} E\{x_{i,P}x_{j,Q}\} - n(n-1)\mu^2\right\}
\end{aligned} \tag{C.11}$$

The two first terms of the sum are the covariance matrix between the two channels P and Q. If the correlation between the two channels at different spatial positions is zero the two last terms disappear. However, when the spatial correlation in the image is different from zero at lags different from zero, the last terms do not disappear. They can be written in function of a "multi-channel spatial correlation" defined as:

$$\begin{aligned}\rho(k;\ P,Q) &= \frac{E\{(x_{i,P}-\mu_P)(x_{i-k,Q}-\mu_Q)\}}{\sqrt{E\{(x_{i,P}-\mu_P)^2\}}\sqrt{E\{(x_{i,P}-\mu_P)^2\}}} \\ &= \frac{E\{(x_{i,P}-\mu_P)(x_{i-k,Q}-\mu_Q)\}}{\sigma_P\sigma_Q} \end{aligned} \tag{C.12}$$

and in a similar way as eq. C.5 it can be shown that:

$$E\{(x_{i,P}-\mu_P)(x_{i-k,Q}-\mu_Q)\} = E\{x_{i,P}x_{i-k,Q}\} - \mu_P\mu_Q \tag{C.13}$$

If the spatial correlation is independent of the interchannel correlation i.e. $\rho(k;\ P,Q) = \rho(k)\rho(P,Q)$ the two last terms in eq. C.11 can be written as:

$$\frac{1}{n}\sum_{i=1}^{n}\sum_{j=1,j\neq i}^{n} E\{x_{i,P}x_{j,Q}\} - n(n-1)\mu^2 = \sigma_P\sigma_Q\sum_{i=1}^{n-1} 2(1-\frac{i}{n})\rho(i)\rho(P,Q) \tag{C.14}$$

Thus finally, noting that $cov(x_P, x_Q) = \sigma_P\sigma_Q\rho(P,Q)$, we get:

$$cov(\overline{x_P},\overline{x_Q}) = \frac{cov(x_P,x_Q)}{n}\left[1+\sum_{i=1}^{n-1} 2(1-\frac{i}{n})\rho(i)\right] \tag{C.15}$$

For the covariance of the mean calculated in a rectangle in a two-dimensional signal we get:

$$cov(\overline{x_P},\overline{x_Q}) = \frac{cov(x_P,x_Q)}{n}\left[1+\sum_{i=1}^{n-1}\sum_{j=1}^{m-1} 2(1-\frac{i}{n})(1-\frac{j}{m})\rho(i,j)\right] \tag{C.16}$$

and thus we obtain the same correction factor as for the variance of mean, but only if the spatial and interchannel correlations are independent. Again this correction factor is only usefull in non-textured regions.

C.3 Correction Factors for the Contour Detectors

For the contour detector based on the Student Test, described in 5.3.1, the correction factor is the square root of the correction factor for the variance. As this detector is applied on the log-intensity image, the average autocorrelation function for log-intensity images is used to calculate the correction factor. For the Hottelings test discussed in 5.4.2 the correction factor is the one for the co-variance matrix, also calculated using the autocorrelation function for log-intensity images. The Levene test (5.4.1) was applied to SLC images, so the correction factor should be determined on the SLC images.

The correction factors were determined based on the spatial correlation functions that were found in 4.2.1 and given in table 4.2 for the SLC image and table 4.3 for the log-intensity image. The results are given in table C.1 for horizontally and vertically oriented 51×11 windows.

Image Type	HH		HV		VV		Average	
	Hor.	Vert.	Hor.	Vert.	Hor.	Vert.	Hor.	Vert.
Complex Image	2.66	3.09	2.68	3.13	2.46	2.96	2.60	3.06
Log-Intensity Image	4.54	4.81	4.74	4.97	5.07	5.32	4.78	5.03

Table C.1: Correction factors for the complex and the Log-Int image

These values can be used to find the theoretical 5 and 1 % false alarm thresholds in uniform regions for the 3 detectors. This is done by multiplying the theoretical threshold with the appropriate correction factor.

For example for the Student test based detector the test statistic follows a $\mathcal{N}(0,1)$ distribution. The 5 % false alarms threshold for uncorrelated observations is thus 1.96. As the test is applied to the log-intensity image and the correction factor is the square root of the correction factor for the variance of the means, this value has to be multiplied with $\sqrt{4.54}$ for horizontal windows and $\sqrt{4.81}$ for vertical windows.

In table C.2 the thresholds are given for vertically and horizontally oriented 51×11 windows. For the Student test based detector the values are given for HH polarisation.

Detector	5 % FA Threshold		1 % FA Threshold	
	Hor.	Vert.	Hor.	Vert.
Student Test based Detector	4.17	4.29	5.47	5.63
Levene Test	5.47	6.44	7.32	8.62
Hotellings Test	12.49	13.14	18.15	19.10

Table C.2: Theoretical 5% and 1% false alarm thresholds taking into account spatial correlation

The correction factors presented above are for 100 % sampling, i.e. when all the pixels in the 11×51 window are used. It is not posssible to calculate a correction factor for random sub-sampling because it is not possible to know a priori which pixels will be chosen in the scanning rectangles. However, for sampling on a fixed grid it is possible to calculate a correction factor by using equations C.8 and C.16 and setting all element of the autocorrelation function to zero except those that correspond to the grid points of the fixed grid.

For the fixed grid defined in fig. 5.12 and using the average autocorrelaton functions presented in 4.2 for the SLC image and table 4.3 for the log-intensity image we get the correction factors given in table C.3 for 51×11 sampling windows.

Image Type	HH		HV		VV		Average	
	Hor.	Vert.	Hor.	Vert.	Hor.	Vert.	Hor.	Vert.
Complex Image	1.11	1.13	1.12	1.14	1.13	1.16	1.12	1.15
Log-Intensity Image	1.038	1.047	1.033	1.040	1.058	1.069	1.044	1.052

Table C.3: Correction factors for the complex and the Log-Int image for Sampling on a Fixed Grid

Appendix D

Implementation of the Fuzzy Classification Method

In sect. 6.2.3 a fuzzy rule-based system was introduced to improve the results of the Cloude decomposition and make the method more easily adaptive to different SAR system. The approach is based on the work of M. Hellmann [63, 60].

In the proposed system the rules are a priori fixed for a given type of vegetation or landcover and a given radar wavelength. The rules are based on physical properties. The actual boundaries of the membership functions depend on more specific properties of the SAR system and need to be adjusted for each type of SAR system.

An image of a given SAR sensor (and a given polarimetric calibration method) should be used to find the boundaries for the membership functions for the different parameters. This is done by delimiting an example of each class to be classified. The values of the different parameters for the different learning objects are represented in fig. D.1 to fig. D.3 as two-dimensional scatter-graphs.

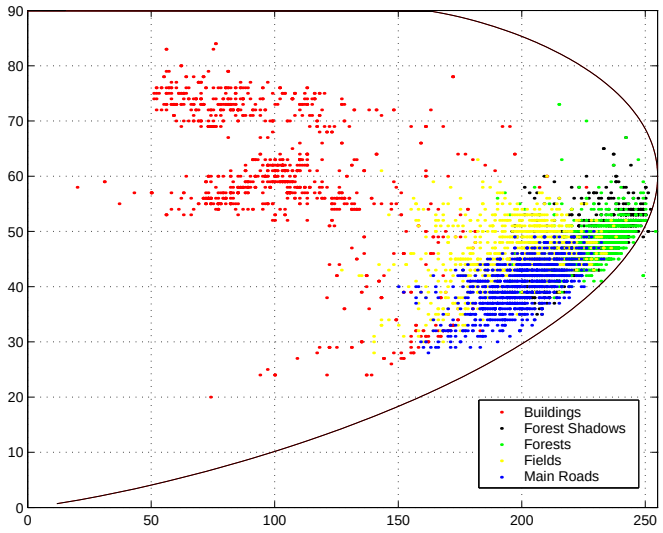

Figure D.1: Scatter graph for H and α

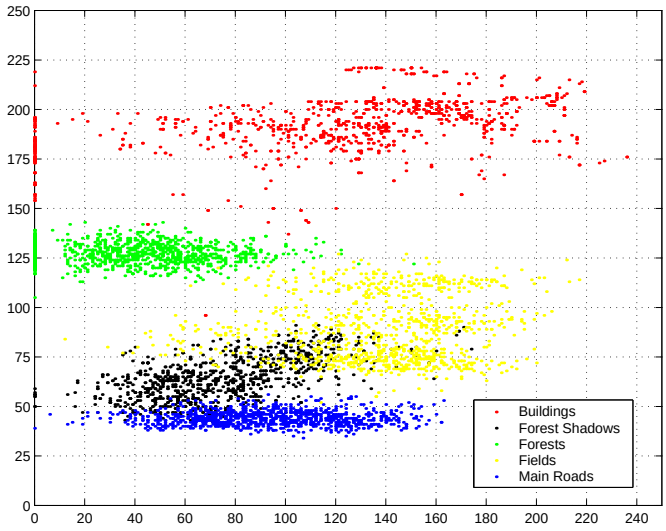

Figure D.2: Scatter graph for λ_1 and Anisotropy

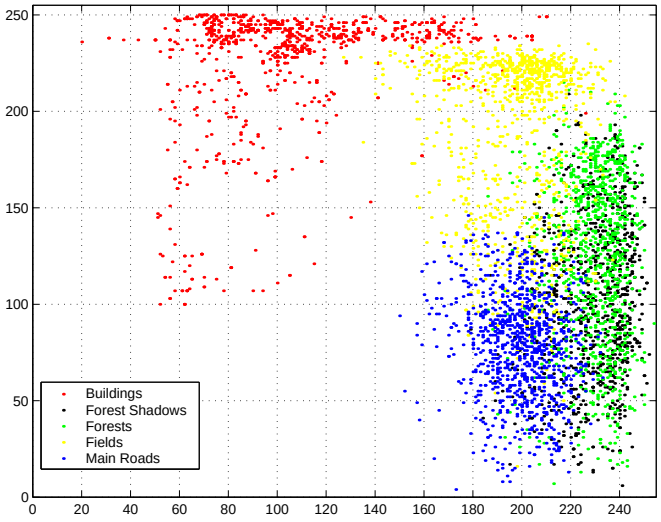

Figure D.3: Entropy H vs. Interferometric Coherence in the set of HH images

These graphs are used to define the borders of the membership functions. The obtained fuzzy membership functions for the different characteristics used in the classification are represented in fig. D.4. Note that the anisotropy, entropy and coherence were all linearly rescaled from their range of possible value to the interval [0..255]. The eigenvalue λ was logarithmically rescaled from the interval $[minimum..maximum]$ found in the image. It some physical range of possible values for λ could be defined, it would be better to use that range in the rescaling. Note that the membership function shown in the figure were derived from image 2 using.

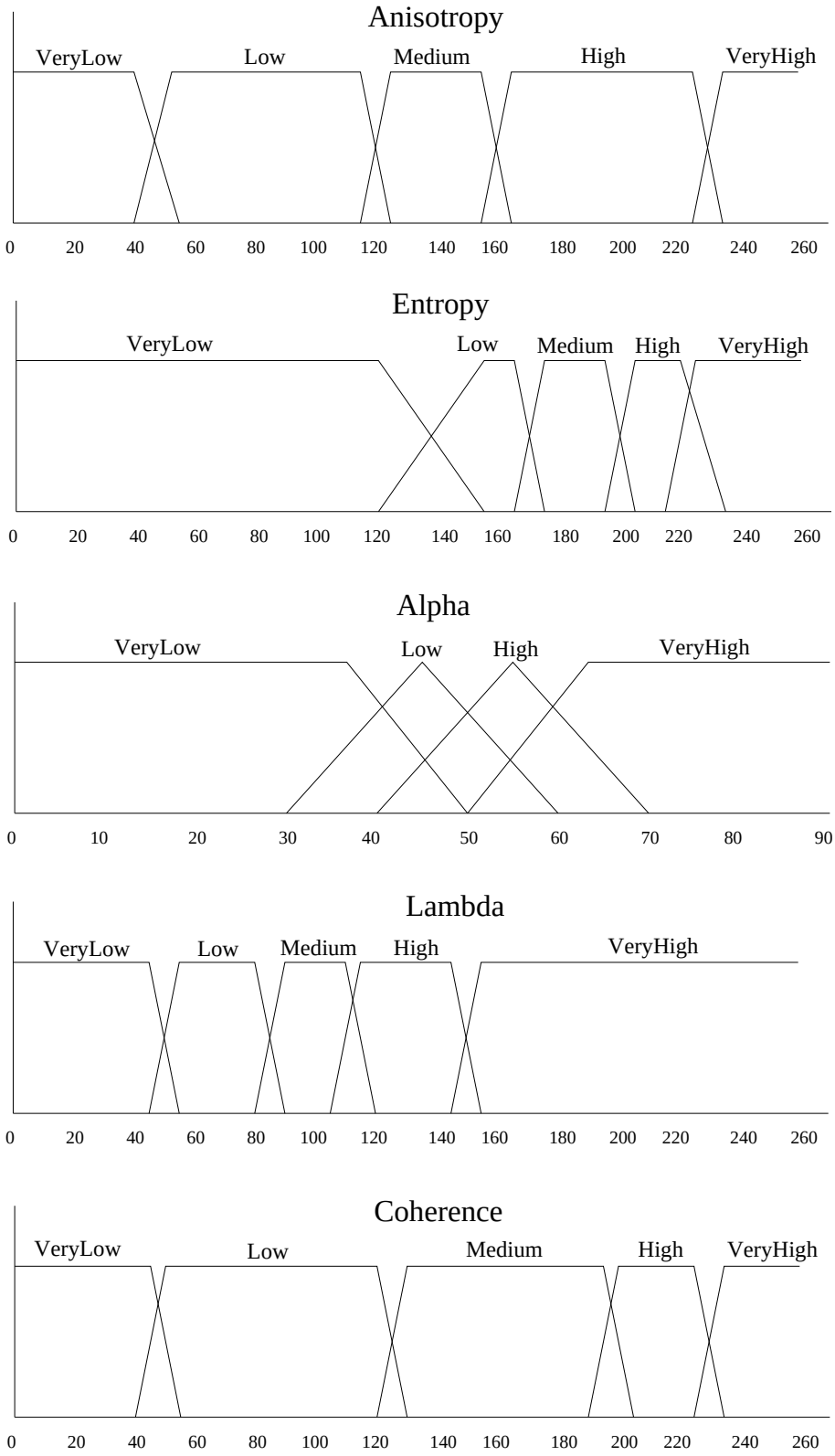

Figure D.4: Input membership functions

Table D.1 presents an overview of the rules used for the fuzzy classification method. The table presents the rules that are applied if all parameters are used. Note that when only a subset of parameters is used, some types of objects become indistinguishable. In that case the rule is assigned to the most important class. This is for example the case for forests and shadows. Only λ_1 allows to distinguish these two classes. In case λ_1 is not used for the classification, shadows will be classified as forests.

A class "reflectors" was added to show that it is possible to detect the trihedral corner reflectors in the scene. Note that one of the field also has the characteristics of a trihedral corner reflector. This is also true for some parts of the roofs of buildings. A possible explanation is the presence of "co-operative specular reflectors", i.e. surfaces that are oriented perpendicular to the incoming radar beam.

Object Type	A	Entropy	α	λ_1	Γ	Color
Forests	VL-L	VH	L-H	H	VL-M	dark green
Buildings	Any	VL	H-VH	VH	M-VH	red
	L-VH	L	H-VH	VH	M-VH	red
Fields	L-H	L-H	VL-H	L-M	L-H	green
Main Roads	L-M	L-H	VL-L	VL	VL-L	grey
Shadows	VL-L	VH	L-H	L	VL-M	blue
Reflectors	M-H	VL	VL	L-VH	VH	Purple

Table D.1: Rules used for the fuzzy classification

The fuzzy classification gives a membership in each pixel of the image for each type of landcover that was defined. A majority rule is then applied to give the final classification result. For a given pixel the majority rule calculates the sum of membership values for each object type in a neighbourhood of that pixel. The pixel is then classified as belonging to the object type that corresponds to the highest sum. We used neighbourhood of 3×3 pixels in the majority rule.